World Journal of Gastroenterology

Submit a Manuscript: https://www.f6publishing.com

World J Gastroenterol 2023 June 28; 29(24): 3793-3806

DOI: 10.3748/wjg.v29.i24.3793

ISSN 1007-9327 (print) ISSN 2219-2840 (online)

ORIGINAL ARTICLE

Basic Study

Transcriptome sequencing and experiments reveal the effect of formyl peptide receptor 2 on liver homeostasis

Hui Liu, Ze-Yu Sun, Hua Jiang, Xu-Dong Li, Yong-Qiang Jiang, Peng Liu, Wen-Hua Huang, Qing-Yu Lv, Xiang-Lilan Zhang, Rong-Kuan Li

Specialty type: Gastroenterology and hepatology

Provenance and peer review: Unsolicited article; Externally peer reviewed.

Peer-review model: Single blind

Peer-review report's scientific quality classification
Grade A (Excellent): 0
Grade B (Very good): B, B
Grade C (Good): 0
Grade D (Fair): 0
Grade E (Poor): 0

P-Reviewer: Heij LR, Germany; Kuboki S, Japan

Received: April 18, 2023
Peer-review started: April 18, 2023
First decision: April 26, 2023
Revised: May 4, 2023
Accepted: May 22, 2023
Article in press: May 22, 2023
Published online: June 28, 2023

Hui Liu, Department of Gastroenterology, Second Hospital of Dalian Medical University, Dalian 116000, Liaoning Province, China

Ze-Yu Sun, Hua Jiang, Yong-Qiang Jiang, Peng Liu, Wen-Hua Huang, Qing-Yu Lv, Xiang-Lilan Zhang, State Key Laboratory of Pathogen and Biosecurity, Institute of Microbiology and Epidemiology, Academy of Military Medical Sciences, Beijing 100071, China

Xu-Dong Li, Microbiology Teaching and Research Office, Anhui Medical University, Hefei 230032, Anhui Province, China

Rong-Kuan Li, Department of Infectious Diseases, Second Hospital of Dalian Medical University, Dalian 116000, Liaoning Province, China

Corresponding author: Rong-Kuan Li, MD, Chief Doctor, Department of Infectious Diseases, Second Hospital of Dalian Medical University, No. 467 Zhongshan Road, Shahekou District, Dalian 116000, Liaoning Province, China. dalianlrk1@163.com

Abstract

BACKGROUND

Formyl peptide receptor 2 (Fpr2) is an important receptor in host resistance to bacterial infections. In previous studies, we found that the liver of $Fpr2^{-/-}$ mice is the most severely damaged target organ in bloodstream infections, although the reason for this is unclear.

AIM

To investigate the role of Fpr2 in liver homeostasis and host resistance to bacterial infections.

METHODS

Transcriptome sequencing was performed on the livers of $Fpr2^{-/-}$ and wild-type (WT) mice. Differentially expressed genes (DEGs) were identified in the $Fpr2^{-/-}$ and WT mice, and the biological functions of DEGs were analyzed by Gene Ontology (GO) and Kyoto Encyclopedia of Genes and Genomes (KEGG) enrichment analysis. Quantitative real time-polymerase chain reaction (qRT-PCR) and western blot (WB) analyses were used to further validate the expression levels of differential genes. Cell counting kit-8 assay was employed to investigate cell survival. The cell cycle detection kit was used to measure the distribution of

cell cycles. The Luminex assay was used to analyze cytokine levels in the liver. The serum biochemical indices and the number of neutrophils in the liver were measured, and hepatic histopathological analysis was performed.

RESULTS

Compared with the WT group, 445 DEGs, including 325 upregulated genes and 120 downregulated genes, were identified in the liver of Fpr2$^{-/-}$ mice. The enrichment analysis using GO and KEGG showed that these DEGs were mainly related to cell cycle. The qRT-PCR analysis confirmed that several key genes (*CycA*, *CycB1*, *Cdc20*, *Cdc25c*, and *Cdk1*) involved in the cell cycle had significant changes. The WB analysis confirmed a decrease in the expression of CDK1 protein. WRW4 (an antagonist of Fpr2) could inhibit the proliferation of HepG2 cells in a concentration dependent manner, with an increase in the number of cells in the G0/G1 phase, and a decrease in the number of cells in the S phase. Serum alanine aminotransferase levels increased in Fpr2$^{-/-}$ mice. The Luminex assay measurements showed that interleukin (IL)-10 and chemokine (C-X-C motif) ligand (CXCL)-1 levels were significantly reduced in the liver of Fpr2$^{-/-}$ mice. There was no difference in the number of neutrophils, serum C-reactive protein levels, and liver pathology between WT and Fpr2$^{-/-}$ mice.

CONCLUSION

Fpr2 participates in the regulation of cell cycle and cell proliferation, and affects the expression of IL-10 and CXCL-1, thus playing an important protective role in maintaining liver homeostasis.

Key Words: Cell cycle; Cell proliferation; Cdk1; Differentially expressed genes; Formyl peptide receptor 2; RNA-sequencing

Core Tip: Formyl peptide receptor 2 (Fpr2) is an important receptor in host resistance to bacterial infection. After Fpr2 deletion, the pathways involved in the cell cycle are affected, the expression of Cdk1 is downregulated, the proliferation activity of HepG2 cells is reduced, and the distribution of cell cycle is abnormal. After Fpr2 deletion, the permeability of the hepatocyte membrane increases, and the expression of interleukin-10 and Chemokine (C-X-C motif) ligand-1 decreases. These changes reflect the important protective effect of Fpr2 in maintaining liver homeostasis.

Citation: Liu H, Sun ZY, Jiang H, Li XD, Jiang YQ, Liu P, Huang WH, Lv QY, Zhang XL, Li RK. Transcriptome sequencing and experiments reveal the effect of formyl peptide receptor 2 on liver homeostasis. *World J Gastroenterol* 2023; 29(24): 3793-3806
URL: https://www.wjgnet.com/1007-9327/full/v29/i24/3793.htm
DOI: https://dx.doi.org/10.3748/wjg.v29.i24.3793

INTRODUCTION

The liver plays an important role in human metabolism and immune homeostasis. Liver dysfunction and liver failure can directly lead to the progression of sepsis and death of patients. Pre-existing liver dysfunction is a risk factor for the progression of infection to sepsis[1]. The liver is an important organ that collects blood from the intestine *via* the portal vein. Once the intestinal barrier becomes dysfunctional, the liver is the first organ to encounter bacteria. The liver collects blood through the hepatic artery, so it is also an important organ involved in the removal of bacteria from the bloodstream in systemic infection[2,3].

As an organ mainly responsible for blood detoxification, the liver plays a key role in removing bacteria and toxins during sepsis. After intravenous injection, the liver captures 65% of bacteria in 10 min and over 80% in 6 h[4]. Two methods of liver clearance have been identified: Rapid and slow. The rapid clearance mainly relies on Kupffer cells to remove bacteria and does not depend on complement-mediated opsonophagocytosis or platelet combinations. The slow clearance ensures that the host not only removes a sufficient number of bacteria to prevent infection and damage but also maintains sufficient bacteria to induce host adaptive immunity. In addition to mesenteric lymph nodes, the liver is another important firewall against bacterial infections in the body[2,5,6].

Formyl peptide receptors (FPRs) are G-protein-coupled receptors that play an important role in host defense and inflammation. The most important biological activity of FPRs is the induction of leukocyte

chemotaxis in infected or injured areas. In addition to chemotaxis, FPRs also mediate phagocytosis, production of reactive oxygen species, and production of various cytokines/chemokines. According to sequence similarity, FPRs are divided into three family members: FPR1, ALX/FPR2, and FPR3. Based on the ability of FPRs to recognize bacterial formylated peptides, they are considered to play an important role in host defense against microbial invasion.

Initially, research on FPRs mainly focused on regulating inflammation, but increasing evidence demonstrated that FPRs can also regulate the host's defense process, including regulating the activation of neutrophils and dendritic cells and participating in host resistance to bacterial infection, tissue damage, and wound healing[7]. Liu *et al*[8] reported that during *Listeria monocytogenes* (*Listeria*) infection, FPRs can quickly recruit the first wave of neutrophils into the infected liver, followed by the second wave of neutrophil accumulation mediated by CXCR2. This discovery challenges the previously reported pattern of host defense against *Listeria*, that is, the receptor toll-like receptor 2 on the host cell is activated by bacterial lipoprotein, and then CXCR2 ligand is produced to induce neutrophil accumulation[9]. In sepsis, the biased expression of chemokine receptors CC chemokine receptor 5 (CCR5) and FPR2 in human and mouse neutrophils leads to the movement of neutrophils guided by CCR5 to aseptic tissue sites, whereas polymorphonuclear neutrophils guided by FPR2 to bacterial infection sites are significantly reduced[10]. Thus, inflammatory but non-functional neutrophils may increase the host's morbidity and mortality, which may be related to infectious injury[11]. The above findings emphasize the importance of FPRs in the host defense against microorganisms.

Our previous research revealed that in group B streptococcus infection, Fpr2 activated the downstream key signal molecules and produced chemokine (C-X-C motif) ligand (CXCL)1/2 to attract neutrophils, indicating that Fpr2, as a chemotactic receptor, could not only attract neutrophils directly, but also indirectly control neutrophil chemotaxis by regulating the production of chemokines to resist infection[12]. The liver is the most important organ in the removal of bacteria, and Fpr2 is an important receptor involved in resisting bacterial infection. However, the effect of Fpr2 on the liver homeostasis remains unclear. In the present study, we evaluated the liver of Fpr2 knockout and wild-type (WT) mice in terms of transcriptome sequencing, histology, immunity, and biochemistry to understand the reason for the antibacterial activity of Fpr2.

MATERIALS AND METHODS

Mice

$Fpr2^{-/-}$ (Fpr2 knockout) mice were purchased from Cyagen Biosciences (Guangzhou, China), who created this model according to previously reported methods[12]. The WT C57BL/6 mice (6-8 wk, 18-20 g body weight) were purchased from Charles River (Beijing, China). These mice were bred in the animal center of the Academy of Military Medical Sciences under specific pathogen free conditions. The animals were acclimatized to laboratory conditions (23 °C, 12 h/12 h light/dark, 50% humidity, and ad libitum access to food and water) for 2 wk, prior to experimentation. All animals were euthanized by isoflurane inhalation for tissue collection. The animal protocol was designed to minimize pain or discomfort to the animals. This research was conducted in compliance with the guidelines for laboratory animal care approved in China. All experimental procedures were approved by the Animal Ethics Committee of the Academy of Military Medical Sciences.

Cell culture

The HepG2 cell line was cultured in a high-glucose DMEM medium (Gibco, Rockville, MD, United States) supplemented with 10% fetal bovine serum (Gibco, Rockville, MD, United States). Cell counting kit-8 (CCK8; APExBIO, United States) assay was employed to investigate cell survival following the manufacturer's instructions. In brief, HepG2 cells were plated in 96-well plates at a density of 3×10^3 cells/well. On the second day, cells were treated with different concentrations of WRW4 [Sangon Biotech (Shanghai) Co., Ltd. China] for 24 h. Then, 10 μL CCK-8 was added to each well and cells were incubated at 37 °C for 2 h. Absorbance was measured at 450 nm using a microplate spectrophotometer (Molecular Devices LLC, Sunnyvale, CA, United States).

The cell cycle detection kit (KeyGEN BioTECH, Nanjing, China) was used to measure the distribution of cell cycles. HepG2 cells were plated in 6-well plates and treated with WRW4 (1 μM) for 24 h. Dimethyl sulfoxide used as a control to dissolve WRW4. Next, cells were collected, washed, and fixed overnight at 4 °C in 70% ethanol. The samples were then incubated with RNase A and propidium in the dark for 30 min and cell cycle distribution was analyzed using flow cytometry.

Total RNA isolation and cDNA library construction

The mice were sacrificed after anesthesia, and the liver was taken for subsequent RNA sequencing. RNA extraction, library preparation, DNA sequencing, and result analysis were conducted by Nevogene Co., Ltd (Beijing, China). Briefly, total RNA was extracted using TRIzol reagent (Invitrogen, Shanghai, China). RNA integrity was assessed using the RNA Nano 6000 Assay Kit on a Bioanalyzer 2100 system (Agilent Technologies, CA, United States).

To select cDNA fragments of 370-420 bp, the library fragments were purified with the AMPure XP system (Beckman Coulter, Beverly, United States). Polymerase chain reaction (PCR) was performed using Phusion High-Fidelity DNA polymerase, Universal PCR primers, and Index (X) Primer. Finally, PCR products were purified (AMPure XP system), and library quality was assessed on the Agilent Bioanalyzer 2100 system. Clustering of the index-coded samples was performed on a cBot Cluster Generation System using TruSeq PE Cluster Kit v3-cBot-HS (Illumina). The library preparations were sequenced on an Illumina Novaseq platform, and 150 bp paired-end reads were generated.

Sequence read quality control, mapping, and counting

After data cleaning (to obtain clean reads with high quality), reads were mapped to the reference genome. Reference genome and gene model annotation files were downloaded from the genome website directly. The index of the reference genome was built using Hisat2 v2.0.5, and paired-end clean reads were aligned to the reference genome using Hisat2 v2.0.5. FeatureCounts v1.5.0-p3 was used to count the number of reads mapped to each gene. Fragments per kilobase millions of each gene were calculated based on the length of the gene and the read counts were mapped to the respective genes.

Differential expression analysis and quantitative real time-PCR validation

Differential expression analysis of the two groups (four biological replicates per group) was performed using the DESeq2 R package (1.20.0). Genes with an adjusted $P < 0.05$ found by DESeq2 were assigned as differentially expressed. Quantitative real time-PCR (qRT-PCR) analysis further validated gene expression patterns. The primers used for qRT-PCR analysis were listed in Table 1.

Enrichment analysis of differentially expressed genes

Gene Ontology (GO) and Kyoto Encyclopedia of Genes and Genomes (KEGG) enrichment analysis of differentially expressed genes (DEGs) were implemented using the ClusterProfiler R package, in which gene length bias was corrected. GO terms with a corrected $P < 0.05$ were considered significantly enriched by DEGs. The ClusterProfiler R package was used to test the statistical significance of DEGs in KEGG enrichment pathways.

Western blotting

The liver tissues were taken and washed three times with phosphate buffer solution, then stored at -80 °C. Total proteins were extracted from the liver using RIPA buffer (Beyotime, Nantong, China), and the concentrations were estimated using the bicinchoninic acid protein assay kit (Pierce, Rockford, IL, United States). Next, 30 μg of protein was separated by sodium dodecyl-sulfate polyacrylamide gel electrophoresis on a 10% gel and transferred to PVDF membranes. The membranes were blocked in 3% nonfat dry milk and then probed with anti-CDK1 antibody (1:2000 dilution; ab32094; Abcam, Cambridge, MA, United States), and anti-beta actin antibody (1:3000; ab8227; Abcam, Cambridge, MA, United States) overnight at 4 °C. On the next day, membranes were incubated with appropriate secondary antibody for 1 h at room temperature. The protein bands were visualized using Amersham Hyperfilm™ ECL reagent (Thermo Fisher Scientific, MA, United States).

Cytokine measurements by the Luminex assay

Fresh liver tissues from the mice were weighed and homogenized. Concentrations of cytokines in the supernatants of the liver were measured by multiplexed Luminex xMAP assay (Cytokine & Chemokine 36-Plex Mouse ProcartaPlex™ Panel 1A; Thermo Fisher Scientific, MA, United States), according to the manufacturer's instructions.

Flow cytometry

The liver tissue was digested into single-cell suspension using type IV collagenase (Sigma-Aldrich, United States). The number of leukocytes in the liver were determined using a BD TruCount system (BD Biosciences, United States). The cells were stained with FITC-anti-mouse Ly6G (Biolegend, San Diego, CA, United States), PerCP-anti-mouse CD45 (Biolegend, San Diego, CA, United States), and PE-anti-mouse CD11b (Biolegend, San Diego, CA, United States) antibodies. All of the above-stained cells were assayed using a BD FACSVerse flow cytometer and data were analyzed using FlowJo software.

Determination of serum biochemical indexes

The blood from mice was collected, and serum was separated by centrifugation (4 °C, 3000 rpm, 10 min). A total of 200 μL serum was obtained and sent to the experimental animal center of the Academy of Military Medical Sciences for the determination of liver biochemical indexes.

Liver histopathology

The liver tissue of mice was fixed with 4% formaldehyde, paraffin sections were prepared, stained with hematoxylin and eosin, and observed and photographed with an Olympus camera system. The image magnifications were 200 × and 400 ×.

Table 1 List of primers used in the study

Primer	Sequences (5' to 3')
CycA-F	GCCTTCACCATTCATGTGGAT
CycA-R	TTGCTCCGGGTAAAGAGACAG
CycB1-F	AGAGCTATCCTCATTGACTGGC
CycB1-R	AACATGGCCGTTACACCGAC
Cdk1-F	AGAAGGTACTTACGGTGTGGT
Cdk1-R	GAGAGATTTCCCGAATTGCAGT
Cdc25c-F	GTTTCAGCACCCAGTTTTAGGT
Cdc25c-R	AGAATGCTTAGGTTTGCCGAG
Cdc20-F	TTCGTGTTCGAGAGCGATTTG
Cdc20-R	ACCTTGGAACTAGATTTGCCAG
Mps1-F	GCAGTGTGACGATTGATTCCA
Mps1-R	TCGGCACAGATTTTAGACAAGC
GAPDH-F	CATGGCCTTCCGTGTTCCTA
GAPDH-R	GCGGCACGTCAGATCCA

Statistical analysis

All data were analyzed using GraphPad Prism (version 8.0; GraphPad Software, La Jolla, CA, United States). Differences between the groups were calculated using an unpaired *t*-test and a log-rank test. Data were shown as mean ± SD. Differences were considered statistically significant at $P < 0.05$.

RESULTS

Identification of DEGs and their GO and KEGG pathway analysis

We used RNA-sequencing to analyze the liver transcriptome of $Fpr2^{-/-}$ mice and compared it with that of WT mice to determine DEGs. Taking $|\log2(\text{fold change})| \geq 1$ and padj ≤ 0.05 as criteria, compared with the WT group, 445 DEGs, including 325 upregulated genes and 120 downregulated genes, were identified in $Fpr2^{-/-}$ mice (Figure 1A). Venn diagram analysis showed that 9578 genes showed identical expression between $Fpr2^{-/-}$ and WT mice. On the other hand, 541 and 371 specific genes were expressed in $Fpr2^{-/-}$ and WT mice, respectively (Figure 1B).

According to the results of the enrichment analysis, 179 GO terms were obtained, including 136 biological processes (BPs), 25 cell component (CC), and 18 molecular function (MF) terms. The results showed that the DEGs were mainly annotated to the cell cycle (Figure 2A). Further GO enrichment analysis of upregulated DEGs showed that a total of 156 GO terms were obtained, including 121 BPs, 25 CC, and 10 MF terms. The BP terms were significantly enriched in mitotic sister chromatid segregation, chromosome segregation, sister chromatid segregation, and nuclear chromosome segregation. The CC terms were significantly enriched in chromosomes, centromeric regions, spindles, mitotic spindles, kinetochores, condensed chromosomes, centromeric regions, and chromosomal regions. The MF terms were significantly enriched in microtubule binding, tubulin binding, and microtubule motor activity (Figure 2B). The results of the GO analysis suggest that the upregulated DEGs are significantly enriched in many phases of cell division. In addition, GO analysis of downregulated DEGs revealed that BP terms were significantly enriched in many BPs related to liver function, such as organic hydroxy compound metabolic process, organic hydroxy compound biosynthetic process, steroid metabolic process, positive regulation of alcohol biosynthetic process, cellular hormone metabolic process, G-protein coupled receptor signaling pathway, and coupled to cyclic nucleotide second messenger (Figure 2C).

Four pathways with significant differences obtained based on KEGG analysis are listed in Table 2. These pathways included cell cycle, neuroactive ligand-receptor interaction, oocyte meiosis, and progesterone-mediated oocyte maturation (Figure 3). Both GO function analysis and KEGG pathway enrichment analysis showed that core DEGs mainly regulated the cell cycle of the liver tissue in Fpr2-deficient mice, which revealed that Fpr2 deficiency may cause cell division cycle disorder to some extent.

Table 2 Kyoto Encyclopedia of Genes and Genomes pathway significant enrichment analysis

Term	Description	Sample number	*P* value	Gene_name
mmu04110	Cell cycle	16/182	0.00009	Cdc20 Ccnb1 Ccnb2 Plk1 Ccna2 Ttk Mad2l1 Wee1 Bub1b Cdk1 Mcm5 Cdkn1a Cdc25c Mcm2 Espl1 Bub1
mmu04080	Neuroactive ligand-receptor interaction	16/182	0.00079	Fpr2 Mtnr1a Gzma P2ry1 Lpar2 Chrna4 Grid1 Gabra3 Adcyap1r1 Vipr1 Calcrl Pth1r Ednra Hcrtr2 Gpr35 P2ry13
mmu04114	Oocyte meiosis	13/182	0.00079	Cdc20 Ccnb1 Ccnb2 Plk1 Mad2l1 Camk2b Adcy1 Ar Cdk1 Cdc25c Adcy7 Espl1 Bub1
mmu04914	Progesterone-mediated oocyte maturation	11/182	0.00132	Ccnb1 Ccnb2 Plk1 Ccna2 Kif22 Mad2l1 Adcy1 Cdk1 Cdc25c Adcy7 Bub1

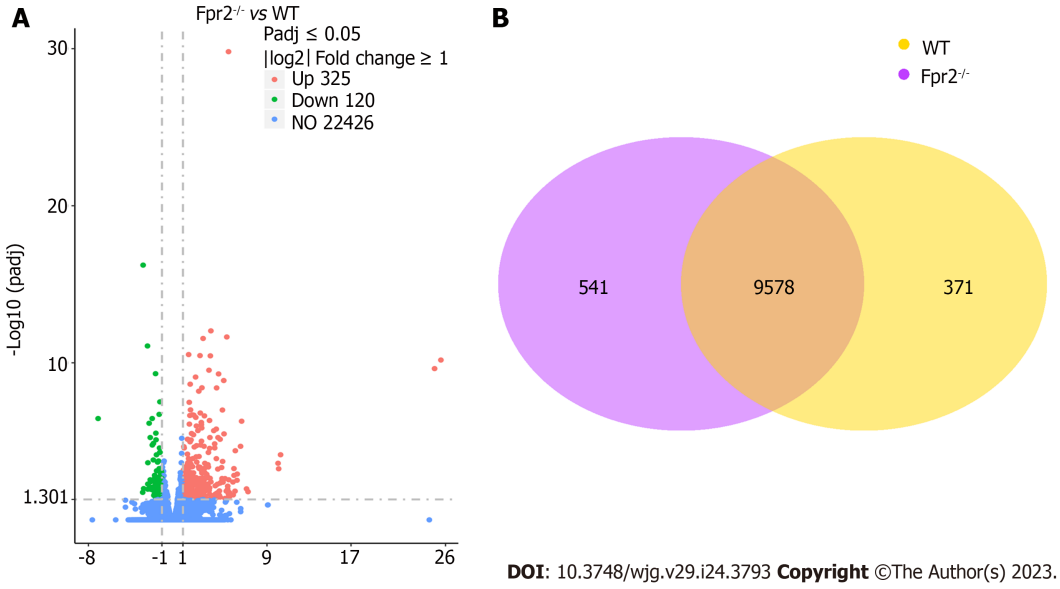

DOI: 10.3748/wjg.v29.i24.3793 **Copyright** ©The Author(s) 2023.

Figure 1 RNA-sequencing analysis of distributions of all differentially expressed genes. A: Volcano map of the distributions of all differentially expressed genes in formyl peptide receptor 2 (Fpr2)$^{-/-}$ and wild-type (WT) mice (n = 4). Red, green, and blue colors respectively represent upregulated genes, downregulated genes, and genes with no difference in expression; B: Venn diagram of gene counts expressed in the Fpr2$^{-/-}$ and WT mice (n = 4). 9578 genes show identical expression between Fpr2$^{-/-}$ and WT mice. 541 and 371 specific genes are expressed in Fpr2$^{-/-}$ and WT mice, respectively. Fpr2: Formyl peptide receptor 2; WT: Wild-type.

Fpr2 participated in the regulation of cell cycle

To further validate the results of RNA-sequencing, we selected several key genes *CycA*, *CycB1*, *Cdc20*, *Cdc25c*, *Mps1*, and *Cdk1*, which are closely related to the cell cycle, for qRT-PCR analysis. The results showed that the expression of *CycA*, *CycB1*, *Cdc20*, and *Cdc25c* was upregulated (Figure 4A), while the expression of *Cdk1* was downregulated in the Fpr2$^{-/-}$ mice (Figure 4B). There was no significant difference in the expression of *Mps1* between Fpr2$^{-/-}$ and WT mice (Figure 4A). The WB analysis further confirmed a decrease in CDK1 expression (Figure 4B). To clarify the impact of Fpr2 deficiency on liver cell proliferation, WRW4, an antagonist of Fpr2, was used to inhibit Fpr2 in the liver cells. CCK-8 further clarified the effect of different concentrations of WRW4 on the proliferation of HepG2 cells. Figure 4C indicates that WRW4 at all concentrations (0.125 μM, 0.25 μM, 0.5 μM, 1.0 μM, and 2.0 μM) inhibited the proliferation of HepG2 cells in a concentration dependent manner. WRW4 at 1 μM was used to analyze the distribution of cell cycles. Flow cytometry analysis showed that the number of cells in G0/G1 phase increased, and the number of cells in S phase decreased (Figure 4D). From the above analysis, it can be surmised that when Fpr2 is absent, some genes involved in cell cycle regulation are affected and these may inhibit cell proliferation by blocking the cell cycle.

Fpr2 maintained the stability of liver cell membrane

Considering that the lack of Fpr2 can lead to disruption of the liver cell cycle, we tested biochemical indicators that reflect liver function. Biochemical indicators related to liver function include determination of the levels of alanine transaminase (ALT), aspartate transaminase (AST), alkaline phosphatase (ALP), lactate dehydrogenase (LDH) and albumin (ALB). In Fpr2$^{-/-}$ mice, we detected higher levels of serum ALT and LDH compared to those in the WT mice, with no significant changes in AST, ALP, and

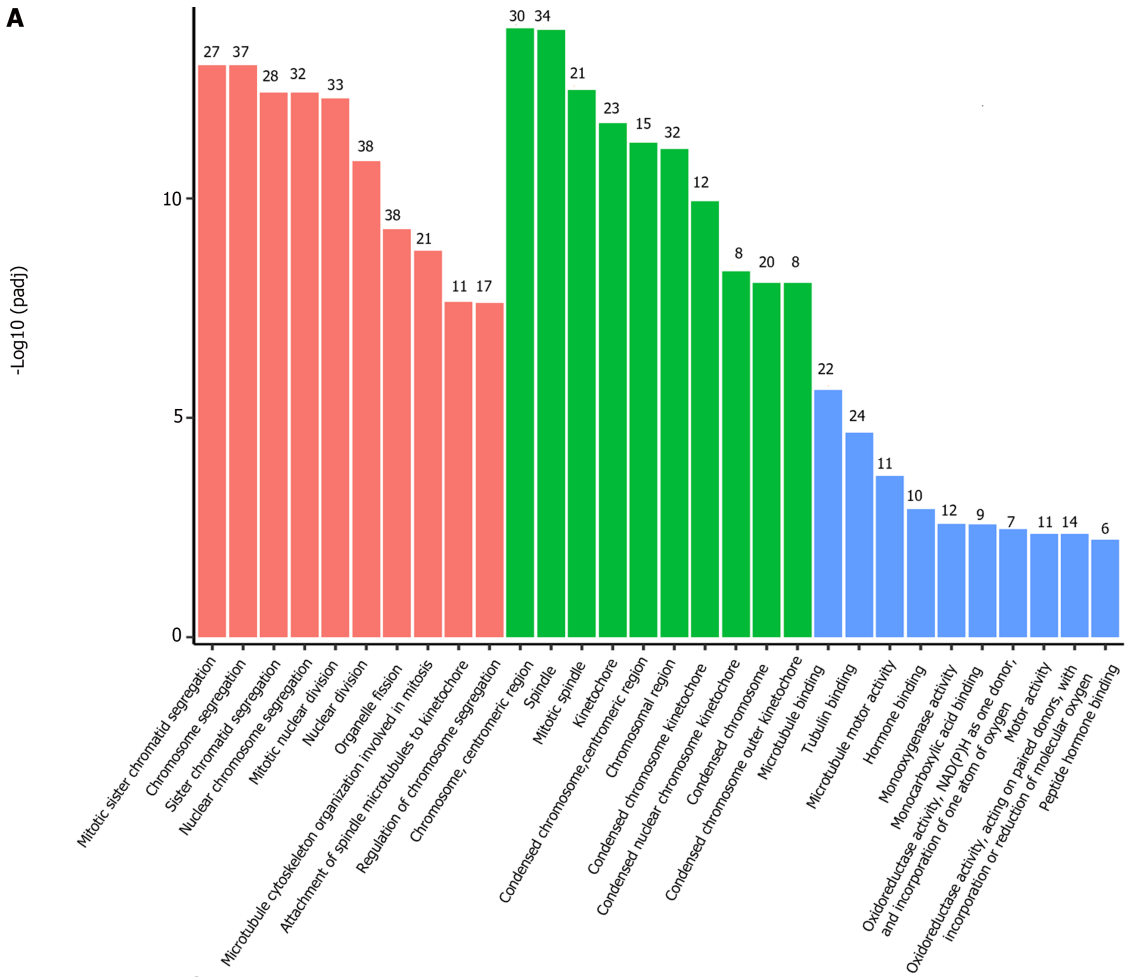
A
-Log10 (padj)
0
5
10
27 37 28 32 33 38 38 21 11 17 30 34 21 23 15 32 12 8 20 8 22 24 11 10 12 9 7 11 14 6
Mitotic sister chromatid segregation
Chromosome segregation
Sister chromatid segregation
Nuclear chromosome segregation
Mitotic nuclear division
Nuclear division
Organelle fission
Microtubule cytoskeleton organization involved in mitosis
Attachment of spindle microtubules to kinetochore
Regulation of chromosome segregation
Chromosome, centromeric region
Spindle
Mitotic spindle
Kinetochore
Condensed chromosome,centromeric region
Chromosomal region
Condensed chromosome kinetochore
Condensed nuclear chromosome kinetochore
Condensed chromosome
Condensed chromosome outer kinetochore
Microtubule binding
Tubulin binding
Microtubule motor activity
Hormone binding
Monooxygenase activity
Monocarboxylic acid binding
Oxidoreductase activity, NAD(P)H as one donor, and incorporation of one atom of oxygen
Motor activity
Oxidoreductase activity, acting on paired donors, with incorporation or reduction of molecular oxygen
Peptide hormone binding

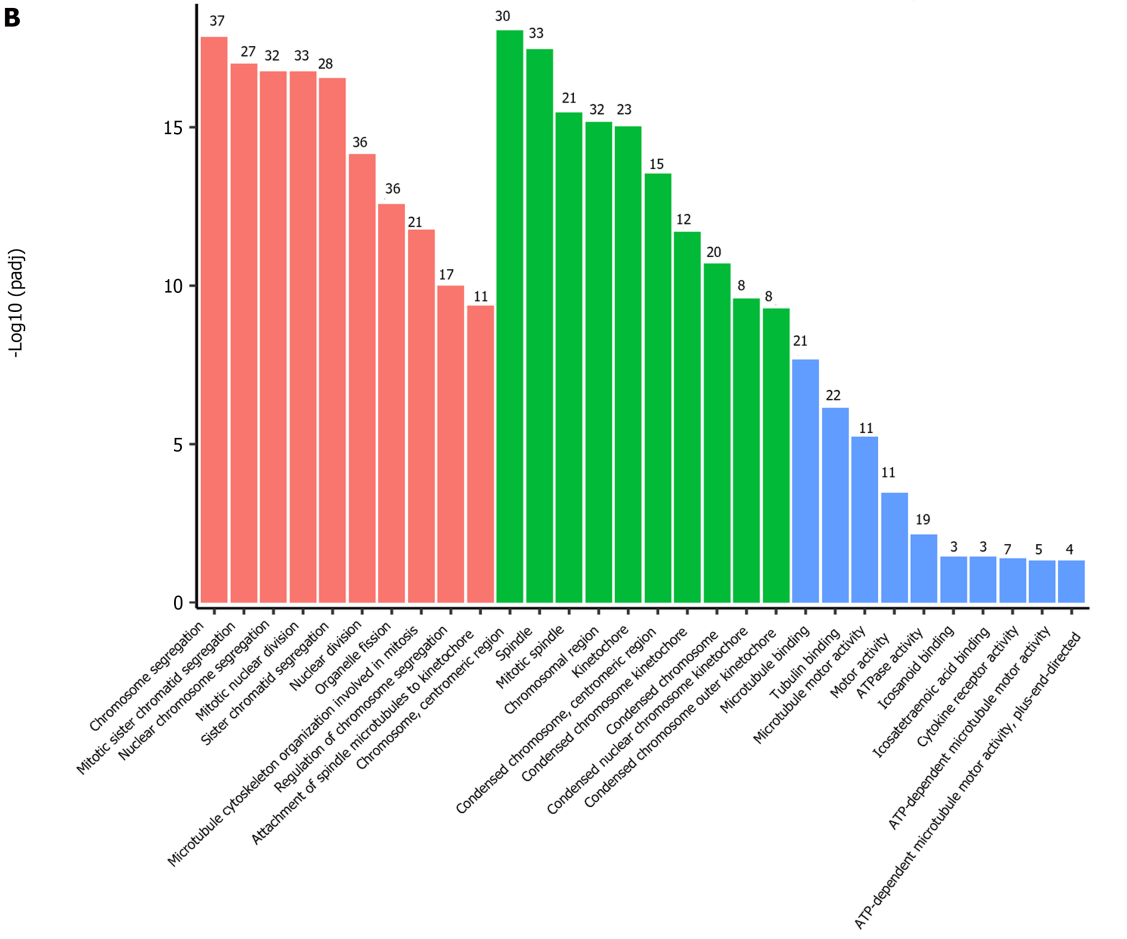
B
-Log10 (padj)
0
5
10
15
37 27 32 33 28 36 36 21 17 11 30 33 21 32 23 15 12 20 8 8 21 22 11 11 19 3 3 7 5 4
Chromosome segregation
Mitotic sister chromatid segregation
Nuclear chromosome segregation
Mitotic nuclear division
Sister chromatid segregation
Nuclear division
Organelle fission
Microtubule cytoskeleton organization involved in mitosis
Regulation of chromosome segregation
Attachment of spindle microtubules to kinetochore
Chromosome, centromeric region
Spindle
Mitotic spindle
Chromosomal region
Kinetochore
Condensed chromosome, centromeric region
Condensed chromosome kinetochore
Condensed chromosome
Condensed nuclear chromosome kinetochore
Condensed chromosome outer kinetochore
Microtubule binding
Tubulin binding
Microtubule motor activity
Motor activity
ATPase activity
Icosanoid binding
Icosatetraenoic acid binding
Cytokine receptor activity
ATP-dependent microtubule motor activity
ATP-dependent microtubule motor activity, plus-end-directed

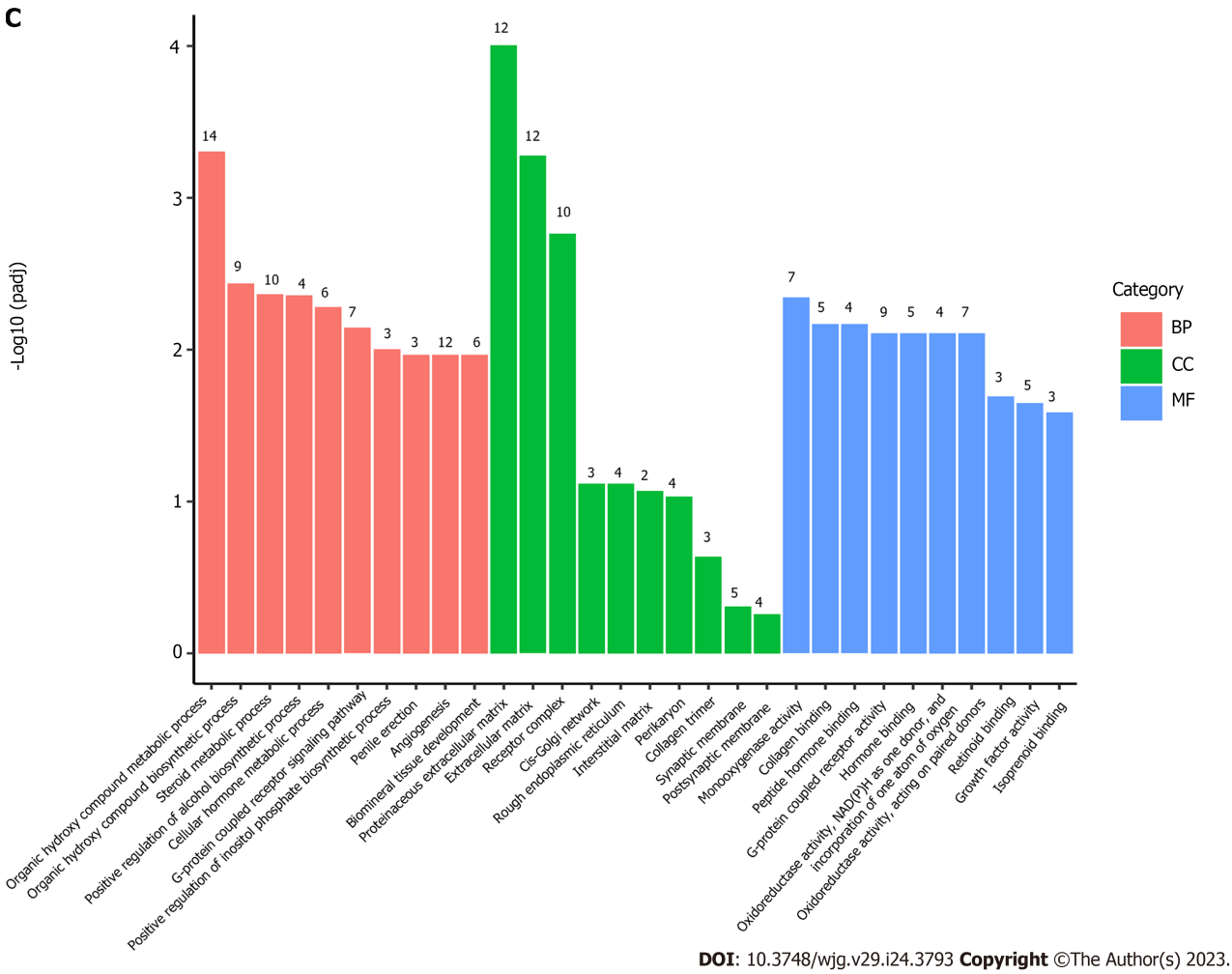

DOI: 10.3748/wjg.v29.i24.3793

Figure 2 Gene Ontology pathway enrichment analysis of differentially expressed genes. The bar graph shows the top 10 (red for biological processes, green for cellular component and blue for molecular function) enriched Gene Ontology pathways. A: Gene Ontology (GO) pathway enrichment analysis of all differentially expressed genes (DEGs); B: GO pathway enrichment analysis of upregulated DEGs; C: GO pathway enrichment analysis of downregulated DEGs. BP: Biological process; CC: Cellular component; MF: Molecular function.

ALB in both mice (Figure 5). When the permeability of the liver cell membrane changes, ALT overflows from the cells into the bloodstream. Therefore, the increase of serum ALT in Fpr2$^{-/-}$ mice suggest that the stability of liver cell membrane is affected.

Fpr2 regulated the expression of interleukin-10 and CXCL-1

In the GO analysis, in addition to cell cycle, ERK1 and ERK2 cascade, myeloid leukocyte activation, and positive regulation of myeloid leukocyte differentiation were also significantly enriched in BP terms, and G-protein coupled receptor activity was significantly enriched in MF terms. These results prompted us to consider whether disruptions in the cell cycle and cell membrane stability may cause inflammation. The Luminex assay was performed to measure the cytokine levels in the liver. The results indicated that in addition to the increased levels of interferon gamma, the levels of interleukin (IL)-4, IL-6, IL-9, IL-12, IL-17A, IL-22, IL-23, IL-27, monocyte chemoattractant protein (MCP)-1, MCP-3, macrophage inflammatory protein (MIP)-1α, MIP-1β, MIP-2, CXCL10, Eotaxin, and tumor necrosis factor-α were decreased at different degrees in the Fpr2$^{-/-}$ mice (Figure 6). The decreases in IL-10, IL-18, and CXCL-1 levels were statistically significant.

Based on the above results, the inflammatory status of the liver was further evaluated. We measured the C-reactive protein (CRP) levels in the peripheral blood and the number of neutrophils in the liver and performed histopathological analysis of the liver. The results showed that there was no significant difference in the CRP levels and the number of neutrophils in the liver between WT and Fpr2 $^{-/-}$ mice (Figures 7A and B), and there was no inflammatory cell infiltration in the histopathology of the liver (Figure 7C). The above results indicate that although the absence of Fpr2 can affect the cell cycle and membrane stability, it does not cause significant inflammation in the liver.

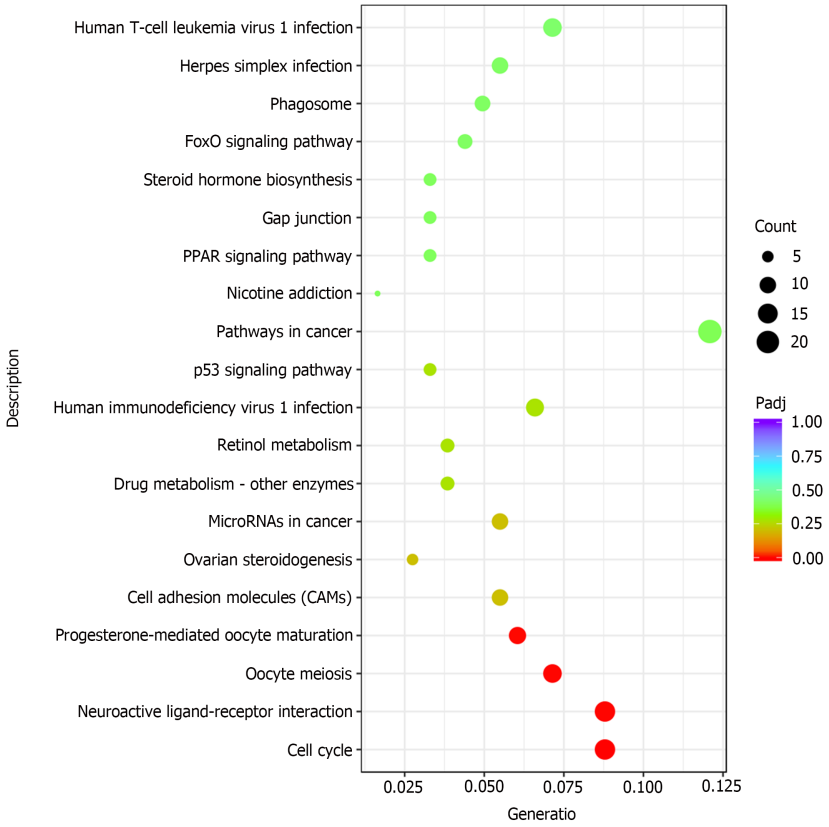

DOI: 10.3748/wjg.v29.i24.3793

Figure 3 Significant enrichment of Kyoto Encyclopedia of Genes and Genomes pathways with differentially expressed genes. The size of the bubble indicates the enrichment score, and the color indicates the significance of the enrichment.

DISCUSSION

In this study, we focused on the effects of Fpr2 on liver homeostasis in mice. According to the results of RNA-sequencing, the deletion of Fpr2 mainly affects the cell cycle of the liver, which is clearly manifested by the significant changes in the expression of several key genes during cell division and enrichment of several related pathways of the cell cycle. The influence of Fpr2 deletion on the cell cycle may be multifaceted. From the perspective of function, DEGs contain many key genes in each stage of the cell cycle (*CycA*, *CycB*, *Cdk1*) and important cell cycle regulatory genes (*Cdc25*, *Cdc20*). In terms of distribution, DEGs are distributed in processes related to spindles, chromatin, and kinetochores. Cdk1 is essential for G1/S and G2/M phase transitions of eukaryotic cell cycle[13]. In $Fpr2^{-/-}$ mice, the expression level of Cdk1 is decreased. When FPR2 of HepG2 cells is blocked by WRW4, the cell proliferation activity decreased, the number of cells in G0/G1 phase increased, and the number of cells in S phase decreased, which indicates that FPR2 can affect cell proliferation by blocking cell cycle.

Most research on FPR2 has focused on its role in the regulation of immune cells in inflammation. Recently, it has also been reported that FPR2 is involved in regulating the migration and proliferation of many types of stem cells. Han *et al*[14] found that the proliferation of hair follicle stem cells and dermal papilla cells in $Fpr2^{-/-}$ mice was significantly reduced, which induced hair loss. Chen *et al*[15] found that $Fpr2^{-/-}$ mice displayed shortened colonic crypts and reduced acute inflammatory responses. This is because intestinal commensal bacteria mediate the proliferation and renewal of epithelial cells through Fpr2. In the present study, we found that the absence of this receptor in liver cells caused abnormal cell cycle. These findings provide evidence for the new function of Fpr2.

Although we found that Fpr2 deficiency can lead to abnormal liver cell cycle and membrane permeability, the infiltration of inflammatory cells in the liver was not observed when probed further. This is consistent with the fact that mice can still grow and reproduce normally with Fpr2 deficiency and do not die due to infection. Therefore, we speculate that these abnormal manifestations after Fpr2 deficiency may be offset by certain protective factors in the body. However, based on our previous research[12], the ability of $Fpr2^{-/-}$ mice to control infection was significantly lower than that of WT mice in the event of bacterial infections, with the liver becoming a severely damaged target organ. Therefore, our current findings may provide an explanation that the imbalance of cellular homeostasis caused by Fpr2 deficiency leads to insufficient defense function of the liver when encountering bacterial infections, making it a target organ for infection damage.

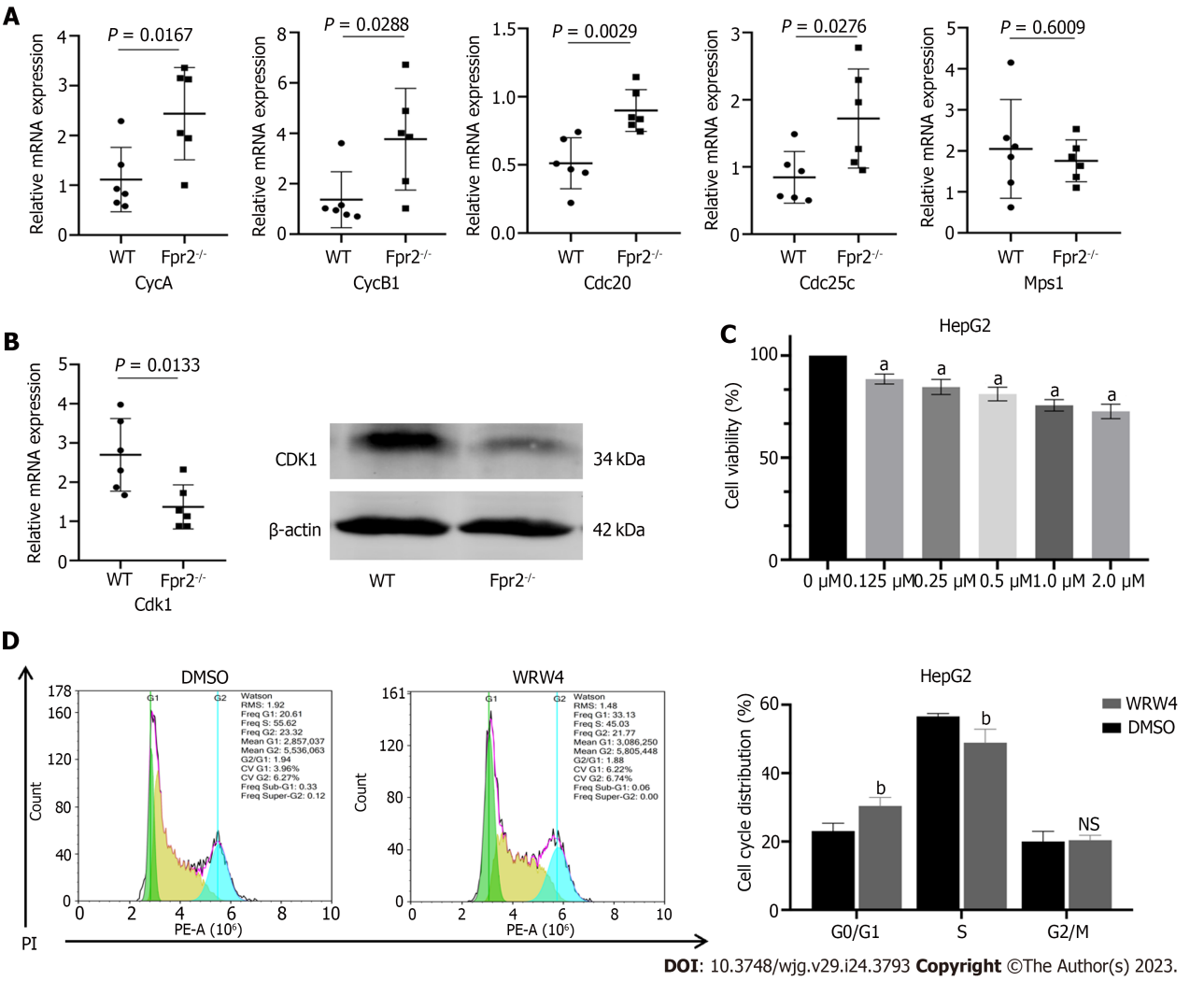

Figure 4 The effect of formyl peptide receptor 2 deletion on cell cycle. A: Quantitative real time-polymerase chain reaction (qRT-PCR) validates the expression of key cell cycle genes regulated by formyl peptide receptor 2 (Fpr2), including *CycA*, *CycB1*, *Cdc20*, *Cdc25c*, and *Mps1* (n = 6). P values are indicated on the graphs; B: qRT-PCR and western blot analyses are used to validate the changes in expression of CDK1; C: The effect of different concentrations of WRW4 on the proliferation activity of HepG2 cells detected by CCK-8 (n = 5); D: The cell cycle distribution of HepG2 cells treated with WRW4 (1 μM) and dimethyl sulfoxide determined by flow cytometry (n = 3). Data are shown as mean ± SD. [a]P < 0.0001 *vs* the 0 μM group; [b]P < 0.05 *vs* the dimethyl sulfoxide group; NS: No significant; Fpr2: Formyl peptide receptor 2; WT: Wild-type; DMSO: Dimethyl sulfoxide.

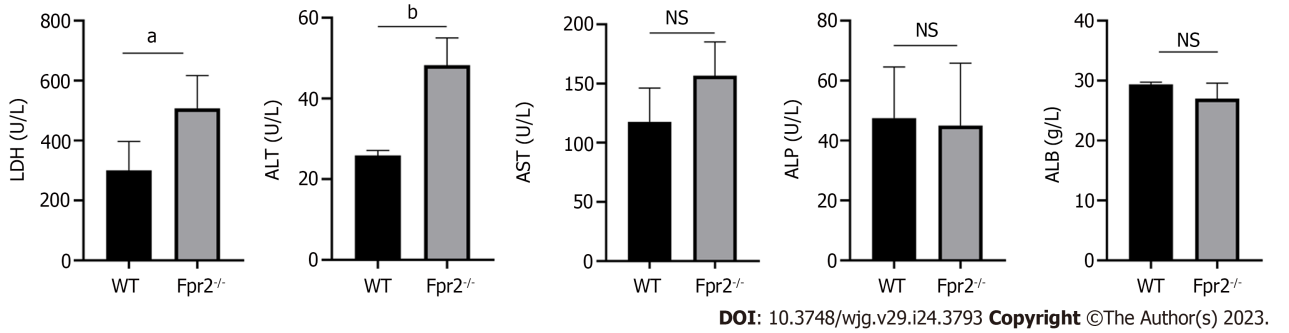

Figure 5 Liver function test in serum of wild-type and formyl peptide receptor 2$^{-/-}$ mice (n = 4). The values are expressed as g/L for albumin levels, and U/L for alanine transaminase, lactate dehydrogenase, aspartate transaminase, and alkaline phosphatase levels. Data are expressed as mean ± SD. [a]P < 0.05, [b] P < 0.01 *vs* the wild-type group; NS: No significant; ALB: Albumin; ALP: Alkaline phosphatase; ALT: Alanine transaminase; AST: Aspartate transaminase; LDH: Lactate dehydrogenase; Fpr2: Formyl peptide receptor 2; WT: Wild-type.

The levels of IL-10 and CXCL-1 were significantly reduced in the liver of Fpr2$^{-/-}$ mice. IL-10 is an important anti-inflammatory factor that can resist the pro-inflammatory effects of other cytokines, thus controlling inflammation. The anti-inflammatory reaction mediated by IL-10 is a fundamental

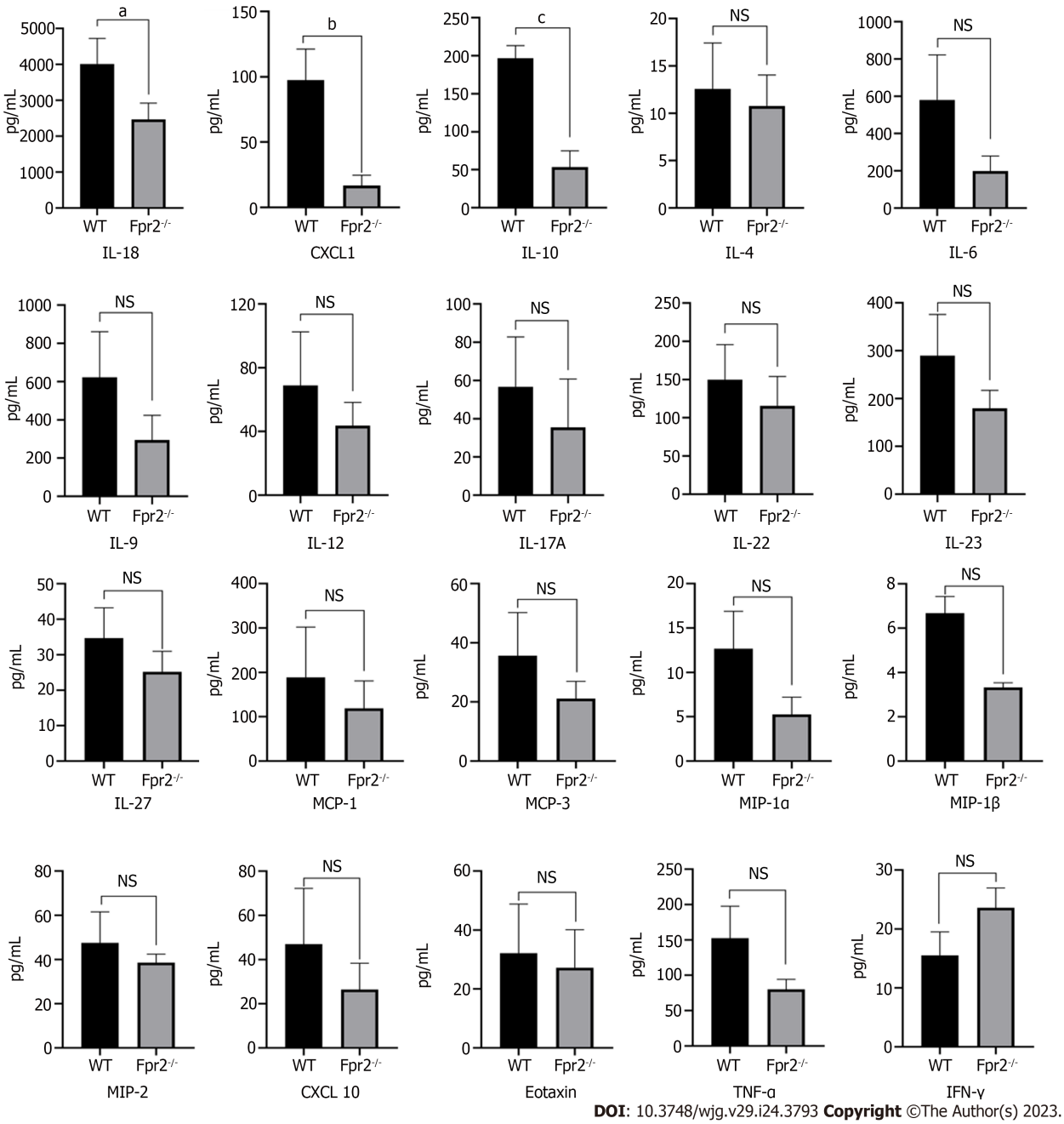

DOI: 10.3748/wjg.v29.i24.3793

Figure 6 Luminex assay analyses cytokines/chemokines concentration in liver of wild-type and formyl peptide receptor 2$^{-/-}$ mice (n = 3). Mean concentration values are shown as normalized to tissue weight. Data are expressed as mean ± SD. $^{a}P < 0.05$, $^{b}P < 0.01$, $^{c}P < 0.001$ *vs* the wild-type group; NS: No significant; CXCL: Chemokine (C-X-C motif) ligand; IFN-γ: Interferon gamma; IL: Interleukin; MCP: Monocyte chemoattractant protein; MIP: Macrophage inflammatory protein; TNF: Tumor necrosis factor; Fpr2: Formyl peptide receptor 2; WT: Wild-type.

homeostatic mechanism that controls the degree and duration of inflammation. IL-10 is an important factor in maintaining immunological tolerance in the liver[16]. IL-10 also plays an important role in liver regeneration and repair[17]. In addition, various cells, such as hepatocytes, endothelial cells, Kupffer cells, and hepatic stellate cells, are involved in the production of IL-10[18]. CXCL-1 is an important chemokine in neutrophils. Our previous research found that the loss of Fpr2 leads to a decrease in the recruitment of neutrophils and weakening of the host's early immune response when resisting infection with *Streptococcus lactis*[12]. Therefore, the decline in repair ability and the decrease in chemotaxis to neutrophils may be another reason why Fpr2$^{-/-}$ mice are seriously injured when infected by bacteria. IL-18 was first discovered in Kupffer cells as a pro-inflammatory factor[19,20]. In Fpr2$^{-/-}$ mice, we observed a decrease in the levels of anti-inflammatory factor IL-10 and pro-inflammatory factor IL-18, and also observed varying degrees of decreases in the levels of other interleukin members, tumor necrosis factors, and chemokines. Considering the cell cycle disruption caused by Fpr2 deficiency, we postulate that the impact of Fpr2 deficiency on cell cycle may interfere with cytokine synthesis, although further validation is needed to test this hypothesis. In short, Fpr2 plays an important role in maintaining liver

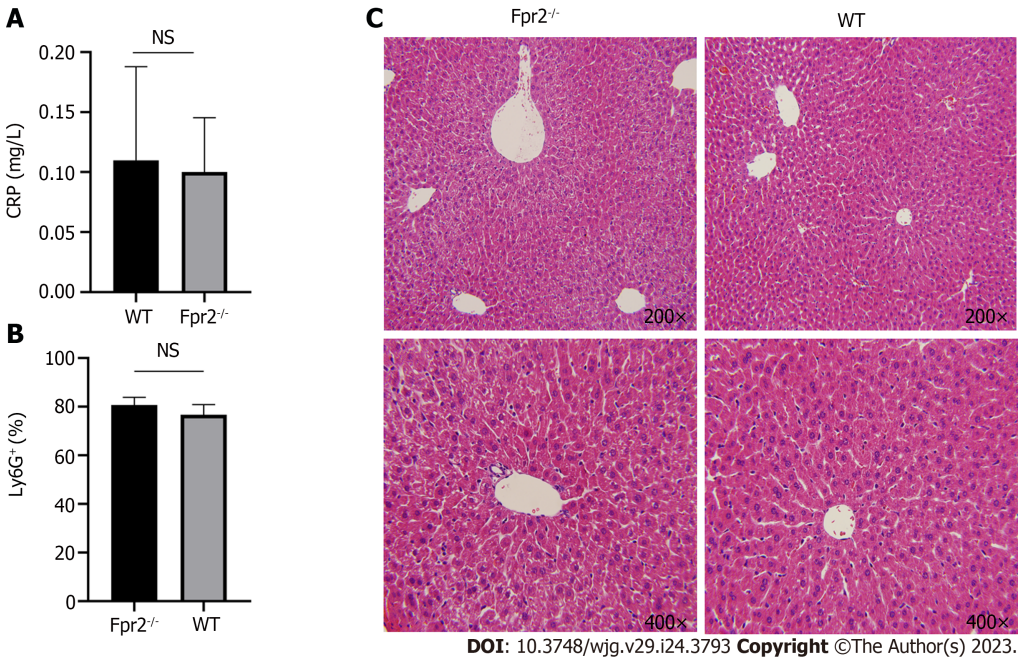

DOI: 10.3748/wjg.v29.i24.3793 **Copyright** ©The Author(s) 2023.

Figure 7 Evaluation of liver inflammation status. A: Serum C-reactive protein level in wild-type (WT) and formyl peptide receptor 2 (Fpr2)$^{-/-}$ mice (n = 4); B: Flow cytometry analysis of the number of neutrophils (% of Ly6G^{+} cells) in the liver of WT and Fpr2$^{-/-}$ mice (n = 3); C: Representative images of hematoxylin-eosin staining of liver tissue sections of Fpr2$^{-/-}$ and WT mice. The image magnification is 200 × and 400 ×. NS: No significant difference. Fpr2: Formyl peptide receptor 2; WT: Wild-type; CRP: C-reactive protein.

homeostasis, which may help the body resist bacterial infections.

Some limitations of this study should be noted. First, we used an immortal liver cell line for our study. Recent studies have reported that mature liver cells located in the middle region of liver lobules are the main contributors to the production of new cells in the entire liver[21,22]. Therefore, it is necessary to further evaluate the regulatory effect of Fpr2 on cell cycle using primary liver cells. Second, further research is required to establish whether Fpr2 regulates cell cycle directly or indirectly.

CONCLUSION

Fpr2 plays an important role in maintaining liver homeostasis by participating in cell cycle regulation. Fpr2 may play a positive role in liver tissue repair and neutrophil chemotaxis by regulating the expression of IL-10 and CXCL-1. Our results provide a basis and novel perspective for further understanding the functional diversity of Fpr2.

ARTICLE HIGHLIGHTS

Research background

Formyl peptide receptor 2 (Fpr2) plays an important role in host's defense and inflammatory response, as it can help the body control bacterial infections. Studies have found that in Fpr2$^{-/-}$ mice, the liver is the most severely damaged target organ in bloodstream infections. However, the reason for this is unclear.

Research motivation

To verify the role of Fpr2 in liver homeostasis, to provide new clues for the decreased ability of the liver to clear bacteria after Fpr2 deficiency, and to provide new ideas for future drug research and development.

Research objectives

To investigate the role of Fpr2 in liver homeostasis.

Research methods

The differentially expressed genes (DEGs) in Fpr2$^{-/-}$ and wild-type (WT) mice were determined by transcriptome sequencing, and the biological functions of DEGs were analyzed by Gene Ontology (GO)

and Kyoto Encyclopedia of Genes and Genomes (KEGG) enrichment analysis. Quantitative real-time polymerase chain reaction (qRT PCR) and western blot (WB) were used to further validate the expression levels of differential genes. The Cell Counting Kit-8 assay was used to study cell proliferation. A cell cycle detection kit was used to measure the distribution of cell cycles. Luminex assay was used to analyze cytokine levels in the liver. A fully automated biochemical analyzer was used to detect the levels of serum biochemical indicators and C-reactive protein in WT and Fpr2$^{-/-}$ mice. The number of neutrophils in the liver was detected by flow cytometry. The histopathology of the liver was analyzed by hematoxylin-eosin staining.

Research results

Transcriptome sequencing showed that, compared with WT group, 445 genes in the liver of Fpr2$^{-/-}$ mice had significant changes in the expression level, including 325 upregulated genes and 120 downregulated genes. The functional enrichment analysis of GO and KEGG indicated that these DEGs were mainly related to cell cycle. qRT-PCR validated that after Fpr2 deletion, the expression levels of *CycA*, *CycB1*, *Cdc20*, and *Cdc25c* genes were upregulated. Both qRT-PCR and WB confirmed a decrease in the expression of CDK1. WRW4 (an antagonist of Fpr2) could inhibit the proliferation of HepG2 cells in a concentration dependent manner. The levels of serum alanine aminotransferase levels increased in Fpr2$^{-/-}$ mice with statistical significance. Luminex assay measurements showed that the expression levels of interleukin (IL)-10, IL-18, and CXCL-1 were significantly reduced in the liver of Fpr2$^{-/-}$ mice.

Research conclusions

Fpr2 may exert a protective effect on the liver by participating in the regulation of cell cycle and proliferation, as well as affecting the expression of IL-10 and CXCL-1.

Research perspectives

Fpr2 plays an important role in maintaining liver homeostasis, and its agonist may be a potential drug against bacterial infection.

FOOTNOTES

Author contributions: Li RK designed the research; Liu H wrote the manuscript; Jiang H, Sun ZY, and Li XD conducted experiments; Liu P, Huang WH, and Lv QY analyzed the data and drew pictures; Jiang YQ and Zhang XL revised the manuscript content; all authors approved the final version of the article.

Supported by the State Key Laboratory of Pathogen and Biosecurity, No. SKLPBS2119 and SKLPBS2212; and the Medical Science Research Project of Dalian, No. 2112015.

Institutional animal care and use committee statement: The animal study was reviewed and approved by the animal center of the Academy of Military Medical Sciences. The protocol for animal handling and experiment was approved by the Institutional Review Board of Academy of Military Medical Science (No: IACUC-DWZX-2022-052).

Conflict-of-interest statement: All the authors report no relevant conflicts of interest for this article.

Data sharing statement: The datasets presented in this study can be found in online repositories. The names of the repository/repositories and accession number(s) can be found below: https://www.ncbi.nlm.nih.gov/, PRJNA923726.

ARRIVE guidelines statement: The authors have read the ARRIVE guidelines, and the manuscript was prepared and revised according to the ARRIVE guidelines.

Country/Territory of origin: China

ORCID number: Hui Liu 0000-0003-4721-560X; Ze-Yu Sun 0009-0007-2720-5750; Hua Jiang 0000-0002-2769-1783; Xu-Dong Li 0009-0007-4750-0212; Yong-Qiang Jiang 0000-0001-7587-830X; Peng Liu 0000-0001-9948-0259; Wen-Hua Huang 0000-0003-4687-2755; Qing-Yu Lv 0009-0000-3620-8522; Xiang-Lilan Zhang 0000-0002-4946-4880; Rong-Kuan Li 0009-0006-9302-7000.

S-Editor: Wang JJ
L-Editor: A

P-Editor: Cai YX

REFERENCES

1 **Yan J**, Li S. The role of the liver in sepsis. *Int Rev Immunol* 2014; **33**: 498-510 [PMID: 24611785 DOI: 10.3109/08830185.2014.889129]

2 **Llorente C**, Schnabl B. Fast-Track Clearance of Bacteria from the Liver. *Cell Host Microbe* 2016; **20**: 1-2 [PMID: 27414492 DOI: 10.1016/j.chom.2016.06.012]

3 **Seki E**, Schnabl B. Role of innate immunity and the microbiota in liver fibrosis: crosstalk between the liver and gut. *J Physiol* 2012; **590**: 447-458 [PMID: 22124143 DOI: 10.1113/jphysiol.2011.219691]

4 **Gonnert FA**, Kunisch E, Gajda M, Lambeck S, Weber M, Claus RA, Bauer M, Kinne RW. Hepatic Fibrosis in a Long-term Murine Model of Sepsis. *Shock* 2012; **37**: 399-407 [PMID: 22266973 DOI: 10.1097/SHK.0b013e31824a670b]

5 **Broadley SP**, Plaumann A, Coletti R, Lehmann C, Wanisch A, Seidlmeier A, Esser K, Luo S, Rämer PC, Massberg S, Busch DH, van Lookeren Campagne M, Verschoor A. Dual-Track Clearance of Circulating Bacteria Balances Rapid Restoration of Blood Sterility with Induction of Adaptive Immunity. *Cell Host Microbe* 2016; **20**: 36-48 [PMID: 27345696 DOI: 10.1016/j.chom.2016.05.023]

6 **Wood NJ**. Liver: the liver as a firewall--clearance of commensal bacteria that have escaped from the gut. *Nat Rev Gastroenterol Hepatol* 2014; **11**: 391 [PMID: 24935420 DOI: 10.1038/nrgastro.2014.90]

7 **Zhang M**, Gao JL, Chen K, Yoshimura T, Liang W, Gong W, Li X, Huang J, McDermott DH, Murphy PM, Wang X, Wang JM. A Critical Role of Formyl Peptide Receptors in Host Defense against Escherichia coli. *J Immunol* 2020; **204**: 2464-2473 [PMID: 32221037 DOI: 10.4049/jimmunol.1900430]

8 **Liu M**, Chen K, Yoshimura T, Liu Y, Gong W, Wang A, Gao JL, Murphy PM, Wang JM. Formylpeptide receptors are critical for rapid neutrophil mobilization in host defense against Listeria monocytogenes. *Sci Rep* 2012; **2**: 786 [PMID: 23139859 DOI: 10.1038/srep00786]

9 **Chen K**, Bao Z, Gong W, Tang P, Yoshimura T, Wang JM. Regulation of inflammation by members of the formyl-peptide receptor family. *J Autoimmun* 2017; **85**: 64-77 [PMID: 28689639 DOI: 10.1016/j.jaut.2017.06.012]

10 **Gobbetti T**, Coldewey SM, Chen J, McArthur S, le Faouder P, Cenac N, Flower RJ, Thiemermann C, Perretti M. Nonredundant protective properties of FPR2/ALX in polymicrobial murine sepsis. *Proc Natl Acad Sci U S A* 2014; **111**: 18685-18690 [PMID: 25512512 DOI: 10.1073/pnas.1410938111]

11 **Diao N**, Zhang Y, Chen K, Yuan R, Lee C, Geng S, Kowalski E, Guo W, Xiong H, Li M, Li L. Deficiency in Toll-interacting protein (Tollip) skews inflamed yet incompetent innate leukocytes *in vivo* during DSS-induced septic colitis. *Sci Rep* 2016; **6**: 34672 [PMID: 27703259 DOI: 10.1038/srep34672]

12 **Sun Z**, Huang W, Zheng Y, Liu P, Yang W, Guo Z, Kong D, Lv Q, Zhou X, Du Z, Jiang H, Jiang Y. Fpr2/CXCL1/2 Controls Rapid Neutrophil Infiltration to Inhibit Streptococcus agalactiae Infection. *Front Immunol* 2021; **12**: 786602 [PMID: 34899755 DOI: 10.3389/fimmu.2021.786602]

13 **Krek W**, Nigg EA. Differential phosphorylation of vertebrate p34cdc2 kinase at the G1/S and G2/M transitions of the cell cycle: identification of major phosphorylation sites. *EMBO J* 1991; **10**: 305-316 [PMID: 1846803 DOI: 10.1002/j.1460-2075.1991.tb07951.x]

14 **Han J**, Lee C, Jung Y. Deficiency of Formyl Peptide Receptor 2 Retards Hair Regeneration by Modulating the Activation of Hair Follicle Stem Cells and Dermal Papilla Cells in Mice. *Dev Reprod* 2021; **25**: 279-291 [PMID: 35141453 DOI: 10.12717/DR.2021.25.4.279]

15 **Chen K**, Liu M, Liu Y, Yoshimura T, Shen W, Le Y, Durum S, Gong W, Wang C, Gao JL, Murphy PM, Wang JM. Formylpeptide receptor-2 contributes to colonic epithelial homeostasis, inflammation, and tumorigenesis. *J Clin Invest* 2013; **123**: 1694-1704 [PMID: 23454745 DOI: 10.1172/JCI65569]

16 **Nguyen NT**, Umbaugh DS, Sanchez-Guerrero G, Ramachandran A, Jaeschke H. Kupffer cells regulate liver recovery through induction of chemokine receptor CXCR2 on hepatocytes after acetaminophen overdose in mice. *Arch Toxicol* 2022; **96**: 305-320 [PMID: 34724096 DOI: 10.1007/s00204-021-03183-0]

17 **Yin S**, Wang H, Park O, Wei W, Shen J, Gao B. Enhanced liver regeneration in IL-10-deficient mice after partial hepatectomy *via* stimulating inflammatory response and activating hepatocyte STAT3. *Am J Pathol* 2011; **178**: 1614-1621 [PMID: 21435447 DOI: 10.1016/j.ajpath.2011.01.001]

18 **Wan S**, LeClerc JL, Schmartz D, Barvais L, Huynh CH, Devière J, DeSmet JM, Vincent JL. Hepatic release of interleukin-10 during cardiopulmonary bypass in steroid-pretreated patients. *Am Heart J* 1997; **133**: 335-339 [PMID: 9060803 DOI: 10.1016/s0002-8703(97)70229-1]

19 **Abbate A**, Toldo S, Marchetti C, Kron J, Van Tassell BW, Dinarello CA. Interleukin-1 and the Inflammasome as Therapeutic Targets in Cardiovascular Disease. *Circ Res* 2020; **126**: 1260-1280 [PMID: 32324502 DOI: 10.1161/CIRCRESAHA.120.315937]

20 **Dinarello CA**. The IL-1 family of cytokines and receptors in rheumatic diseases. *Nat Rev Rheumatol* 2019; **15**: 612-632 [PMID: 31515542 DOI: 10.1038/s41584-019-0277-8]

21 **He L**, Pu W, Liu X, Zhang Z, Han M, Li Y, Huang X, Han X, Liu K, Shi M, Lai L, Sun R, Wang QD, Ji Y, Tchorz JS, Zhou B. Proliferation tracing reveals regional hepatocyte generation in liver homeostasis and repair. *Science* 2021; **371** [PMID: 33632818 DOI: 10.1126/science.abc4346]

22 **Wei Y**, Wang YG, Jia Y, Li L, Yoon J, Zhang S, Wang Z, Zhang Y, Zhu M, Sharma T, Lin YH, Hsieh MH, Albrecht JH, Le PT, Rosen CJ, Wang T, Zhu H. Liver homeostasis is maintained by midlobular zone 2 hepatocytes. *Science* 2021; **371** [PMID: 33632817 DOI: 10.1126/science.abb1625]

Published by **Baishideng Publishing Group Inc**
7041 Koll Center Parkway, Suite 160, Pleasanton, CA 94566, USA
Telephone: +1-925-3991568
E-mail: bpgoffice@wjgnet.com
Help Desk: https://www.f6publishing.com/helpdesk
https://www.wjgnet.com